

Synthesis and Optical Properties of Novel Unsymmetrical Conjugated Dendrimers

Zhonghua Peng,* Yongchun Pan, Bubin Xu, and Jianheng Zhang

Contribution from the Department of Chemistry, University of Missouri–Kansas City, 5100 Rockhill Road, Kansas City, Missouri 64110

Received February 25, 2000

Abstract: The first unsymmetrical conjugated dendrimer was synthesized using a rather simple approach that involves only one synthon and two sets of reaction conditions. This dendrimer shows broad absorption in the UV and visible range and possesses an intrinsic energy gradient from the outside branches to the core, naturally suggesting itself as a potentially efficient light harvesting material.

Dendrimers possess a multibranched structure that radiates out from a central core.¹ Such a dendritic structure not only represents a fundamentally new molecular architecture, it also offers an enormous opportunity for creating new functional materials.¹ One characteristic of dendritic molecules is the presence of numerous peripheral end groups that all converge to a single core. Such a structure naturally suggests itself as a molecular antenna suitable for transferring energy or electrons from the surface to the core. Indeed, several elegant light-harvesting dendrimers have been reported by Fréchet,² Moore,³ and others.⁴ Fréchet's dye-labeled dendrimer utilizes flexible poly(aryl ether)s as the dendritic skeleton. The energy transfer from the peripheral dye to the center dye takes place through a dipole–dipole interaction (Förster Energy Transfer), which is distance dependent. Efficient energy transfer is achieved with dendrimers up to the fourth generation.² Moore reported a series of rigid phenylacetylene-based dendrimers with a fluorescent perylene chromophore at the locus.³ One particularly novel design is the so-called “extended” dendrimer that possesses consecutively increasing conjugation length toward the center of the molecule, thus creating an energy gradient from the outside branches to the inside branches. Such a dendrimer could act as an energy funnel.

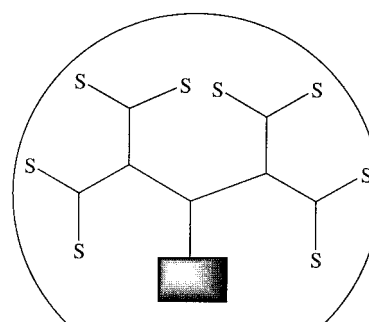
However, all these light-harvesting systems utilize symmetrical dendrimers: dendrimers with equivalent branches. As a matter of fact, almost all the dendrimers (not just those developed for light harvesting applications) studied so far have symmetrical structures.¹ This is due partly to the chemists' fascination with molecular regularity and partly to the ease in

(1) (a) Newkome, G. R.; Moorefield, C. N.; Vögtle, F. *Dendritic Molecules: Concepts, Syntheses, Perspectives*; VCH: Weinheim, 1996. (b) Fréchet, J. M. J.; Hawker, C. J. In *Synthesis and Properties of Dendrimers and Hyperbranched Polymers, Comprehensive Polymer Science*, 2nd Suppl.; Aggarwal, S. L., Russo, S., Eds.; Pergamon: Oxford, 1996. (c) Fischer, M.; Vögtle, F. *Angew. Chem., Int. Ed. Engl.* **1999**, *38*, 884–905. (d) Smith, D. K.; Diederich, F. *Chem. Eur. J.* **1998**, *4* (8), 1353–1361. (e) Tomalia, D. A.; Naylor, A. M.; Goddard, W. A., III *Angew. Chem., Int. Ed. Engl.* **1990**, *29*, 138–175. (f) Zeng, F.; Zimmerman, S. C. *Chem. Rev.* **1997**, *97*, 1681–1712.

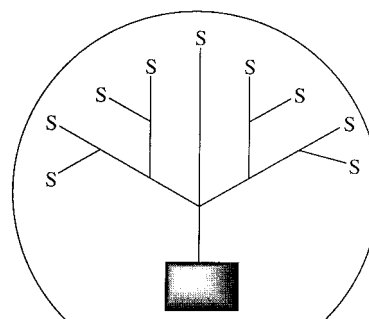
(2) Gilat S. L.; Adronov, A.; Fréchet, J. M. J. *Angew. Chem., Int. Ed. Engl.* **1999**, *38*, 1422–1427.

(3) (a) Devadoss, C.; Bharathi, P.; Moore, J. S. *J. Am. Chem. Soc.* **1996**, *118*, 9635. (b) Shortreed, M. R.; Swallen, S. F.; Shi, Z.; Tan, W.; Xu, Z.; Devadoss, C.; Moore, J. S.; Kopelman, R. *J. Phys. Chem. B* **1997**, *101*, 6318.

(4) (a) Balzani, V.; Campagna, S.; Denti, G.; Juris, A.; Serroni, S.; Venturi, M. *Acc. Chem. Res.* **1998**, *31*, 26–34. (b) Stewart, G. M.; Fox, M. A. *J. Am. Chem. Soc.* **1996**, *118*, 4354–4360.



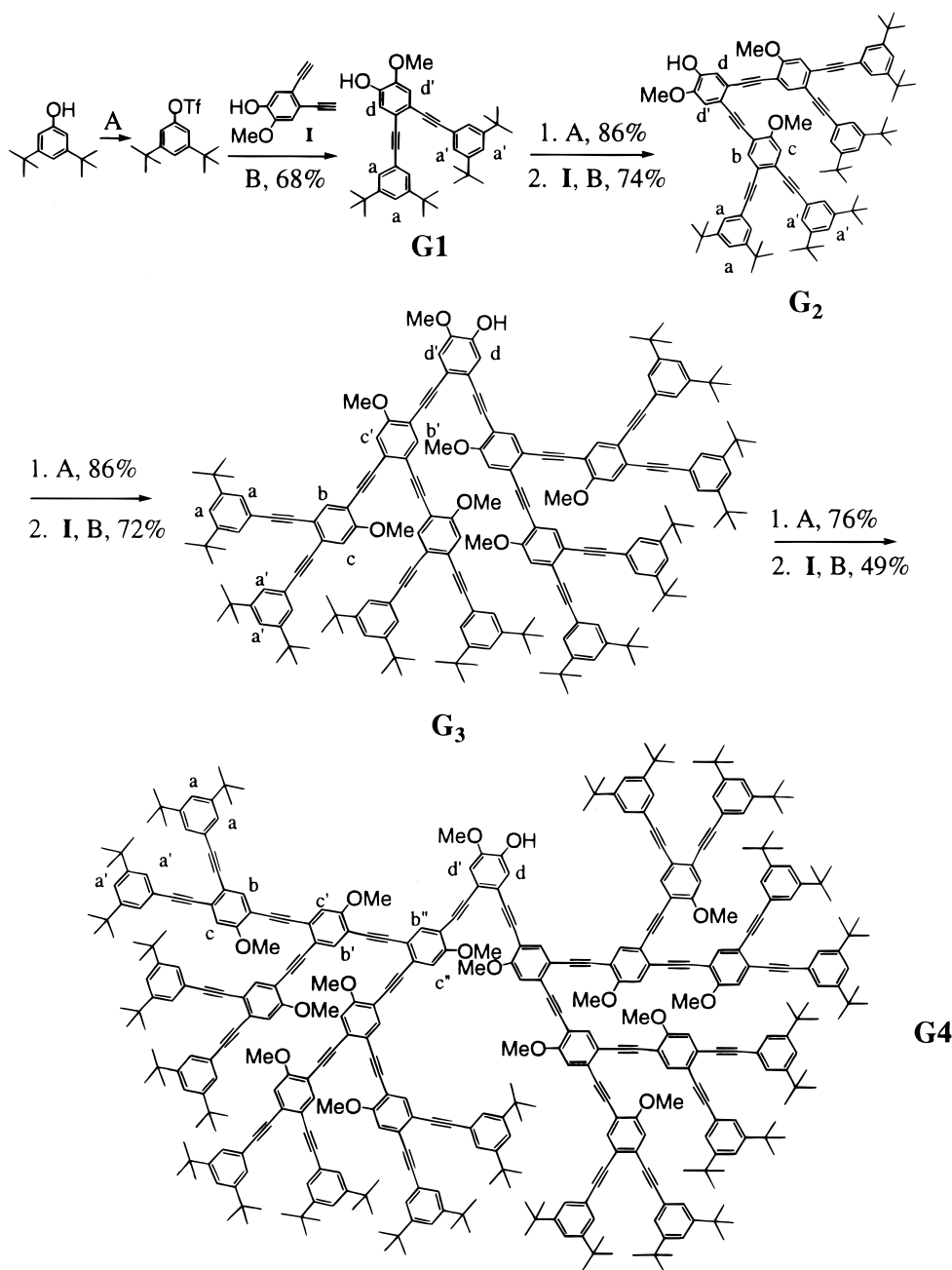
A: A symmetrical dendron



B: An unsymmetrical dendron

Figure 1. Models of dendrimers with symmetrical branches (A) and tree-like branches (B).

synthesis. A model of such dendrimers is shown in Figure 1 as model **A**. Trees in nature, however, prefer unsymmetrical branches, which presumably allow better transportation of nutrients among leaves and roots, as well as sub-branches. This can be easily understood by inspecting the two models shown in Figure 1. For symmetrical dendrimers, communication between peripheral groups and the core has to go through each sub-branch. For tree-like dendrimers (Model **B** in Figure 1), however, shortcuts such as the trunk or main branches exist so that the core can reach the end groups directly. We thus believe that dendrimers with unsymmetrical branches may be better materials if signal communication between dendrimer periphery segments and the core is required. In other words, tree-like

Scheme 1. Synthetic Sequence to Conjugated Unsymmetrical Dendrimers

dendrimers may be better candidates as light-harvesting antennae and energy-transferring funnels.

To materialize and demonstrate the above concept, we recently synthesized a new type of conjugated dendrimer based on meta- and para-linked phenylacetylenes (taking the core as the reference point for describing the branching). Two features are unique to this new dendritic structure: different branches exhibit different conjugation lengths, which results in a broad absorption spectral range, and conjugation lengths increase from the outside branches to the core, which generates an intrinsic energy gradient pointing inward. Thus, such a dendrimer could act as an extremely efficient light-harvesting material by funneling a broad wavelength range of light to the energy trap at the locus. In addition, this dendrimer possesses a phenol

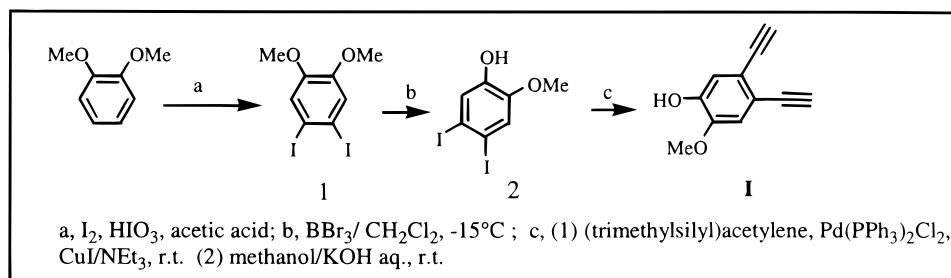
hydroxyl group at the core which should allow the attachment of a variety of structural units to the dendritic core, resulting in an array of novel new functional dendrimers. This paper reports the detailed synthesis and optical properties of these dendrimers.

Experimental Section

Scheme 1 shows the synthetic approach to various generation dendrimers. The building block molecule, compound **I**, was synthesized according to Scheme 2. All chemicals were purchased from Aldrich Chemical Co. and used as received unless otherwise stated.

4,5-Diiodo-2-methoxyphenol (2): A 17.1 mL sample of BBr_3 (1 M solution in CH_2Cl_2) was added dropwise to the solution of compound **1** (20 g, 51.3 mmol) in CH_2Cl_2 (25 mL) at -15°C (ice-salt bath). After being stirred for 1 h at room temperature, the mixture was poured into water. The organic layer was separated, washed with water, and then dried over sodium sulfate. The solvent was removed and the

Scheme 2. Synthesis of 4,5-Diethynyl-2-methoxyphenol



resulting residue was subjected to chromatographic separation. The desired product (compound **2**) was obtained in 43% yield (8.5 g, mp 80–82 °C). ¹H NMR (CDCl₃, ppm): δ 7.39 (s, 1H, Ar–H), 7.24 (s, 1H, Ar–H), 5.58 (s, 1H, OH), 3.86 (s, 3H, OCH₃). ¹³C NMR (CDCl₃, ppm): δ 147.4, 146.4, 125.0, 121.1, 96.9, 94.9, 56.4.

2-Methoxy-4,5-di(trimethylsilylethynyl)phenol: A 2.36 g (24 mmol) sample of trimethylsilylacetylene was added to a mixture containing compound **2** (3.76 g, 10 mmol), Pd(PPh₃)₂Cl₂ (0.281 g, 0.4 mmol), CuI (0.152 g, 0.8 mmol), and trimethylamine (30 mL) at room temperature. The resulting mixture was stirred for 5 h and then the solids were separated from the solution by filtration. The filtrate was concentrated and then dissolved in CH₂Cl₂. The resulting solution was washed with an aqueous HCl solution and then with water. The organic layer was separated and dried over Na₂SO₄. The crude product was purified by chromatography eluting with 5:1 hexane/ethyl acetate to give the title compound as a white powder (2.6 g, 82%). Mp: 60–62 °C. ¹H NMR (CDCl₃, ppm): δ 6.99 (s, 1H, Ar–H), 6.91 (s, 1H, Ar–H), 5.68 (s, 1H, OH), 3.88 (s, 3H, OCH₃), 0.26 (s, 18H, SiMe₃).

4,5-Diethynyl-2-methoxyphenol (Compound I): A 20 mL sample of aqueous KOH solution (1 N) was added to the solution containing 2.6 g of 2-methoxy-4,5-di(trimethylsilylacetylene)phenol and 20 mL of methanol at room temperature. The mixture was stirred at room temperature for 1 h. After removal of the majority of the solvent, the residue was treated with an aqueous HCl solution. The resulting solution was extracted with methylene chloride. The organic layer was collected and the solvent was evaporated. The resulting mixture was purified by chromatography on silica gel using 3:1 hexane/ethyl acetate as the eluent to yield compound **I** as a brownish yellow crystal (1.1 g, 80%). Mp: 91–93 °C. ¹H NMR (CDCl₃, ppm): δ 7.04 (s, 1H, Ar–H), 6.95 (s, 1H, Ar–H), 5.79 (s, 1H, OH), 3.88 (s, 3H, OCH₃), 3.26 (s, 2H). ¹³C NMR (CDCl₃, ppm): δ 146.9, 146.3, 118.9, 118.5, 117.6, 114.5, 82.2, 81.9, 79.9, 79.5, 56.3.

3,5-Di-tert-butylphenyl trifluoromethanesulfonate: A 16.4 g sample of trifluoromethanesulfonic anhydride (58.2 mmol) was added slowly to the solution of 3,5-di-tert-butylphenol (10 g, 48.5 mmol) in 20 mL of pyridine at 0 °C. The resulting mixture was warmed to room temperature and stirred for 3 h, then poured into water. The aqueous solution was extracted with CH₂Cl₂. The organic layer was washed with an aqueous HCl solution and then dried over Na₂SO₄. After stripping off the solvent, the residue was purified through a short silica gel column eluting with 8:1 hexane/ethyl acetate to yield the title compound as a colorless oil (15.3 g, 93%). ¹H NMR (CDCl₃, ppm): δ 7.44 (s, 1H, Ar–H), 7.09 (s, 2H, Ar–H), 1.33 (s, 18H, t-Bu). ¹³C NMR (CDCl₃, ppm): δ 153.9, 150.0, 122.4, 121.6, 116.6, 115.7, 35.4, 31.5.

4,5-Di(3',5'-di-tert-butylphenylethynyl)-2-methoxyphenol (G1): A 2.4 g sample of triethylamine (24 mmol) was added to the mixture of compound **I** (1.03 g, 6 mmol), 3,5-di-tert-butylphenyl trifluoromethanesulfonate (4.08 g, 12 mmol), Pd(PPh₃)₂Cl₂ (0.250 g, 0.36 mmol), and 20 mL of DMF at room temperature. The resulting mixture was stirred at 70 °C for 4 h under nitrogen. After cooling to room temperature, the mixture was poured into water and extracted with CH₂Cl₂. The organic layer was washed with an aqueous HCl solution and then dried over MgSO₄. The crude product was purified by chromatography using silica gel (230–400 mesh) eluting with 5:1 hexane/ethyl acetate to yield **G1** as a pale powder (1.1 g, 68% yield according to the amount of triflate that reacted; triflate (2.0 g) was recovered after the reaction). Mp: 138–140 °C. ¹H NMR (CDCl₃, ppm): δ 7.37 (s, 6H, H_a), 7.12 (s, 1H, H_d), 7.05 (s, 1H, H_{d'}), 5.74 (s, 1H, OH), 3.93 (s, 3H, OCH₃),

1.26 (s, 36H, t-Bu). ¹³C NMR (CDCl₃, ppm): δ 150.9, 146.6, 145.8, 126.0, 122.5, 120.0, 118.7, 117.8, 113.8, 93.5, 93.1, 87.3, 86.9, 56.2, 34.9, 31.5.

4,5-Di(3',5'-di-tert-butylphenylethynyl)-2-methoxyphenyl trifluoromethanesulfonate (G1-OTf): A 0.472 g sample of trifluoromethanesulfonic anhydride (1.67 mmol) was added to a solution containing **G1** (0.765 g, 1.40 mmol) and 10 mL of pyridine at 0 °C. The resulting mixture was stirred for 3 h. The workup procedure was similar to that of 3,5-di-tert-butylphenyl trifluoromethanesulfonate. **G1-OTf** (0.82 g) was obtained (86%). Mp: 157–159 °C. ¹H NMR (CDCl₃, ppm): δ 7.41 (s, 2H, Ar–H), 7.40 (s, 1H, Ar–H), 7.38 (s, 2H, Ar–H), 7.36 (s, 2H, Ar–H), 7.20 (s, 1H, Ar–H), 3.97 (s, 3H, OCH₃), 1.26 (s, 36H, t-Bu). ¹³C NMR (CDCl₃, ppm): δ 151.2, 138.0, 127.7, 126.2, 126.1, 125.8, 123.7, 123.4, 122.0, 121.7, 121.5, 119.5, 116.4, 116.1, 96.6, 95.1, 85.9, 85.4, 56.7, 35.0, 31.5.

The synthetic procedure for **G2**, **G3**, and **G4** is similar to that of **G1**, and the procedure for the synthesis of **G2-OTf** and **G3-OTf** is similar to that of **G1-OTf**.

G2: Yield: 74%. Mp: 150–152 °C. ¹H NMR (CDCl₃, ppm, see Scheme 1 for the labeling): δ 7.81 (s, 1H, H_b), 7.80 (s, 1H, H_{b'}), 7.38 (s, 6H, H_a), 7.36 (s, 6H, H_a), 7.15 (s, 1H, H_d), 7.07 (s, 3H, H_{d'} and H_c), 5.74 (s, 1H, OH), 3.96 (s, 3H, OCH₃), 3.89 (s, 3H, OCH₃), 3.88 (s, 3H, OCH₃), 1.25 (m, 72H, t-Bu). ¹³C NMR (CDCl₃, ppm): δ 159.3, 151.0, 146.9, 146.1, 137.2, 127.1, 126.1, 126.0, 123.3, 122.9, 122.5, 122.1, 119.7, 118.8, 118.3, 118.1, 114.1, 113.8, 113.5 (Ar–C); 96.4, 94.4, 94.0, 93.8, 88.0, 87.6, 87.3, 86.4 (alkyne); 56.3 (OCH₃), 34.9, 31.5 (t-Bu). Anal. Calcd for C₈₉H₁₀₀O₄: C, 86.64, H, 8.17. Found: C, 86.57, H, 8.08. MALDI-TOF for C₈₉H₁₀₀O₄ calcd 1232.76, found 1232.24.

G2-OTf: Yield: 86%. Mp: 140–142 °C. ¹H NMR (CDCl₃, ppm): δ 7.81 (s, 1H, Ar–H), 7.79 (s, 1H, Ar–H), 7.44 (s, 1H, Ar–H), 7.38 (s, 6H, Ar–H), 7.35 (s, 6H, Ar–H), 7.21 (s, 1H, Ar–H), 7.08 (s, 1H, Ar–H), 7.07 (s, 1H, Ar–H), 3.98 (s, 3H, OCH₃), 3.88 (s, 3H, OCH₃), 1.25 (m, 72H, t-Bu). ¹³C NMR (CDCl₃, ppm): δ 159.5, 159.4, 151.3, 151.0, 138.2, 137.4, 137.2, 128.1, 127.7, 127.2, 126.1, 125.9, 123.4, 123.0, 122.5, 122.1, 119.1, 118.9, 116.2, 113.8, 112.8 (Ar–C); 97.0, 96.8, 94.0, 93.9, 92.6, 92.2, 90.5, 89.6, 87.2, 86.3, 86.2 (alkyne); 56.7, 56.4 (OCH₃), 34.9, 31.5 (t-Bu).

G3: Yield: 78%. Mp: 180 °C dec. ¹H NMR (CDCl₃, ppm, see Scheme 1 for the labeling): δ 7.83 (s, 4H, H_b), 7.80 (s, 2H, H_{b'}), 7.37 (s, 12H, H_a), 7.34 (s, 12H, H_a), 7.16 (s, 1H, H_d), 7.10 (s, 2H, H_c), 7.06 (s, 5H, H_{d'} and H_c), 5.97 (s, 1H, OH), 3.97 (s, 3H, OCH₃), 3.91 (s, 6H, OCH₃), 3.89 (s, 12H, OCH₃), 1.25 (m, 144H, t-Bu). ¹³C NMR (CDCl₃, ppm): δ 159.4, 150.9, 146.9, 146.2, 137.5, 137.2, 128.2, 127.7, 127.2, 126.7, 126.1, 125.9, 123.3, 122.9, 122.5, 122.1, 119.7, 118.8, 118.3, 113.9, 113.8, 113.4, 112.9 (Ar–C), 96.7, 96.4, 94.6, 94.3, 94.1, 93.8, 93.7, 93.4, 90.9, 88.7, 88.3, 87.9, 87.6, 87.2, 86.4, 86.3 (alkyne), 56.4, 56.3 (OCH₃), 34.9, 31.7 (t-Bu). Anal. Calcd for C₁₈₉H₂₀₄O₈: C, 87.19, H, 7.90. Found: C, 87.22, H, 7.87. MALDI-TOF for **G3**, calcd for C₁₈₉H₂₀₄O₈ 2601.56, found 2600.42.

G3-OTf: Yield: 76%. Mp: 174–176 °C. ¹H NMR (CDCl₃, ppm): δ 7.85 (s, 4H, Ar–H), 7.80 (s, 2H, Ar–H), 7.46 (s, 1H, Ar–H), 7.37 (s, 12H, Ar–H), 7.34 (s, 12H, Ar–H), 7.07–7.12 (m, 7H, Ar–H), 4.00 (s, 3H, OCH₃), 3.91 (s, 6H, OCH₃), 3.89 (s, 12H, OCH₃), 1.25 (m, 144H, t-Bu). ¹³C NMR (CDCl₃, ppm): δ 159.6, 159.4, 159.3, 150.9, 138.2, 137.5, 137.2, 127.9, 127.6, 127.3, 126.1, 125.9, 123.3, 123.0, 122.5, 122.1, 118.9, 118.8, 118.5, 114.1, 113.8, 113.3, 113.2, 113.1, 112.8, 112.7 (Ar–C); 96.8, 96.5, 94.0, 93.9, 93.8, 93.2, 93.1, 92.8,

92.4, 91.4, 91.2, 90.9, 89.5, 88.6, 88.5, 87.3, 87.2, 86.4, 86.2 (alkyne); 56.7, 56.4 (OCH₃), 34.9, 31.5 (t-Bu).

G4: Yield: 49%. Mp: 230 °C dec. ¹H NMR (CDCl₃, ppm, see Scheme 1 for the labeling): δ 7.79–7.88 (m, 14H, H_b, H_{b'}, and H_{b''}), 7.36 (s, 24H, H_{a'}), 7.33 (s, 24H, H_a), 7.16 (s, 1H, H_d), 7.06–7.11 (m, 15H, H_{d'}, H_c, H_{c'}, and H_{c''}), 5.75 (s, 1H, OH), 3.89 (br, 45H, OCH₃), 1.25 (m, 288H, t-Bu). ¹³C NMR (CDCl₃, ppm): δ 159.7, 159.6, 159.4, 159.3, 150.9, 146.9, 146.1, 137.8, 137.5, 137.2, 127.7, 127.2, 126.8, 126.1, 126.0, 123.3, 122.9, 122.5, 122.2, 118.8, 118.8, 118.4, 114.1, 113.9, 113.8, 113.5, 113.4, 113.3, 112.9 (Ar-C); 96.7, 96.4, 94.6, 94.4, 94.4, 94.3, 94.2, 94.1, 93.9, 93.8, 93.7, 93.5, 93.3, 91.2, 90.9, 88.5, 88.3, 87.4, 87.3, 86.5, 86.3 (alkyne); 56.4 (OCH₃), 34.9, 31.5 (t-Bu). Anal. Calcd for C₃₈₉H₄₁₂O₁₆: C, 87.44, H, 7.77. Found: C, 87.56, H, 7.79. MALDI-TOF for **G4**, calcd for C₃₈₉H₄₁₂O₁₆ 5339.14, found 5339.10.

Characterization. The ¹H NMR spectra were collected on a Bruker 250 MHz FT NMR spectrometer. A Hewlett-Packard 8452A diode array spectrophotometer was used to record the UV/vis absorption spectra. Photoluminescence properties were measured using a Shimadzu RF-5301PC spectrofluorophotometer.

Results and Discussion

The synthesis of compound **I** is shown in Scheme 2. 4,5-Diiodo-1,2-dimethoxybenzene was synthesized from 1,2-dimethoxybenzene.⁵ The monodemethylation of compound **1** was accomplished by slow addition of 0.33 equiv of BBr₃ and the product was separated by chromatography. The yield is 43%. Direct iodination of 2-methoxyphenol to generate compound **2** with a variety of common iodination reagents⁶ such as I₂/HIO₃, I₂/Bu₄N⁺-SO₃OOSO₃⁻NBu₄, I₂/HgCl₂, ICl, and (Me₃N⁺CH₂-Ph)(ICl₂)⁻/CaCO₃ has not been successful. Palladium-catalyzed coupling (Sonogashira reaction⁷) of compound **2** with trimethylsilylacetylene, followed by desilylation with potassium hydroxide, generates compound **I** in 61% yield.

The conversion of phenol to triflate is trivial, and high yield is obtained in each case (over 75%). The cross-coupling of triflate with acetylene could be carried out on compound **I** without the protection of the hydroxy group,⁸ greatly simplifying the synthetic process. Good yields (over 65%) are obtained for the syntheses of **G1**, **G2**, and **G3**. Even for **G4**, a reasonable yield of 49% is obtained.

G1 to **G4** are soluble in common organic solvents such as CHCl₃, CH₂Cl₂, THF, etc. Their structures are confirmed by NMR, elemental analysis, and MALDI-TOF experiments (see Experimental Section). As shown in Figure 2, the ¹H NMR spectra of all four dendrons show clearly a single peak in the range of 5.70–6.00 ppm, which can be assigned to the hydroxyl proton in the core. No signals corresponding to the acetylene protons are observed, which indicates that both terminal alkynes coupled with the aryl triflate. The peaks of methoxy protons appear between 3.88 and 3.97 ppm. For **G1**, only one single peak corresponding to methoxy protons appears at 3.93 ppm. For **G2**, there are two well-separated peaks at 3.96 and 3.89 ppm with an integration ration of 1 to 2. These two peaks can be assigned to the methoxy protons on the core phenyl ring and on the branch phenyl ring, respectively. The peak at 3.89

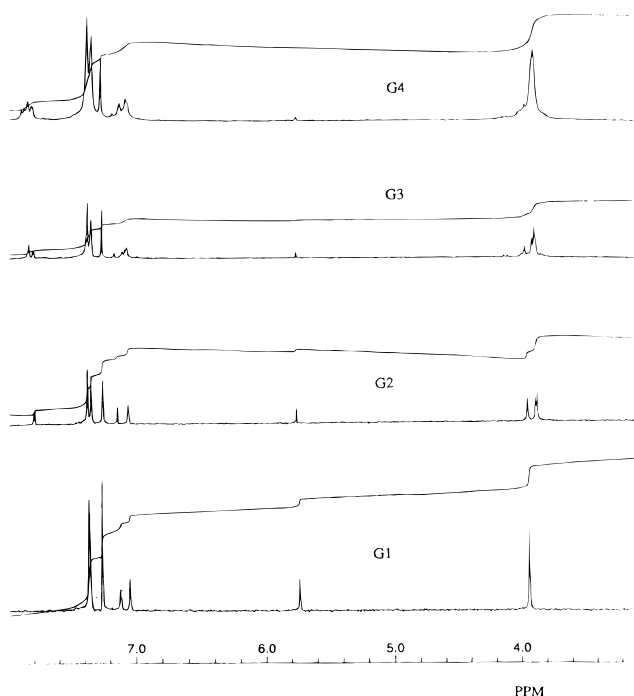


Figure 2. ¹H NMR spectra of **G1–G4**.

ppm is composed of two strongly overlapped but still distinguishable peaks at 3.89 and 3.88 ppm, indicating the inequivalency of the two sets of methoxy groups in the two center phenyl rings. For **G3**, three peaks are observed at 3.97, 3.91, and 3.88 ppm, with the later two again severely overlapped. For **G4**, all the methoxyl protons are merged to one broad peak at 3.75 ppm. The aromatic region of the ¹H NMR spectra of **G1–G4** can be separated into three regions. Chemical shifts at 7.75–7.95 ppm are due to protons at the ortho position of both ethynyl substituents in the central phenyl rings (protons labeled b, b', and b'' in Scheme 1). **G1** shows no signal in this region, while **G2** shows two close signals. For **G3**, two well-separated sets of peaks at 7.83 and 7.80 ppm are observed with an integration ratio of 2:1. The two sets of signals are due to protons in the two layers of phenyl rings (protons b and b', respectively). For **G4**, broad and multiple peaks are observed in this region. The second region shows chemical shifts at 7.30–7.40 ppm, which are the signals of the peripheral aryl protons. **G1** shows one peak, while **G2**, **G3**, and **G4** all show two peaks with equal intensity in this region. The third region shows chemical shifts at 7.00–7.20 ppm, which are due to aromatic protons in the core and aromatic protons at the ortho position of the methoxy group in the central phenyl rings (protons labeled c, c', and c'' in Scheme 1).

These dendritic molecules show drastically different optical properties from meta-linked conjugated dendrimers. As shown in Figure 3, the lowest excitation energy shifts to the red with increasing generations. The absorption edges for **G1**, **G2**, **G3**, and **G4** are 360, 420, 450, and 460 nm, respectively. Apparently, the effective conjugation length continues to increase with increasing dendrimer size, albeit the steric congestion resulting from the ortho linkage prevents the phenyl rings from adopting a planar geometry. Another important feature of this series of dendrimers is that the core electronically communicates with the periphery through two extended conjugated arms. Other branches maintain cross-conjugation with these two extended conjugation arms. We anticipate that this type of dendrimer may be a better energy transfer funnel than meta-linked phenylacetylene dendrimers, due to the fact that this system provides a

(5) Xu, B.; Zhang, J.; Peng, Z. *Synth. Met.* **1999**, *107*, 47–51.

(6) (a) Bao, Z.; Chen, Y.; Cai, R. B.; Yu, L. *Macromolecules* **1993**, *26*, 5281. (b) Bachki, A.; Foubelo, F.; Yus, M. *Tetrahedron* **1994**, *50* (17), 5139–46. (c) Orito, K.; Hatakeyama, T.; Takeo, M.; Sugimoto, H. *Synthesis* **1995**, *10*, 1273. (d) Yusubov, M. S.; Filimonov, V. D.; Jin, H.-W.; Chi, K.-W. *Bull. Korean Chem. Soc.* **1998**, *19* (4), 400–401. (e) Yang, S. G.; Kim, Y. H. *Tetrahedron Lett.* **1999**, *40* (33), 6051–6054.

(7) Takahashi, S.; Kuroyama, Y.; Sonogashira, K.; Hagihara, N. *Synthesis* **1980**, *8*, 627.

(8) (a) Chen, Q. Y.; Yang, Z. Y. *Tetrahedron Lett.* **1986**, *27*, 1171. (b) Arcadi, A.; Cacchi, S.; Marinelli, F. *Tetrahedron Lett.* **1989**, *30*, 2581. (c) Evans, K. L.; Prince, P.; Huang, E. T.; Boss, K. R.; Gandour, R. D. *Tetrahedron Lett.* **1990**, *31*, 6753.

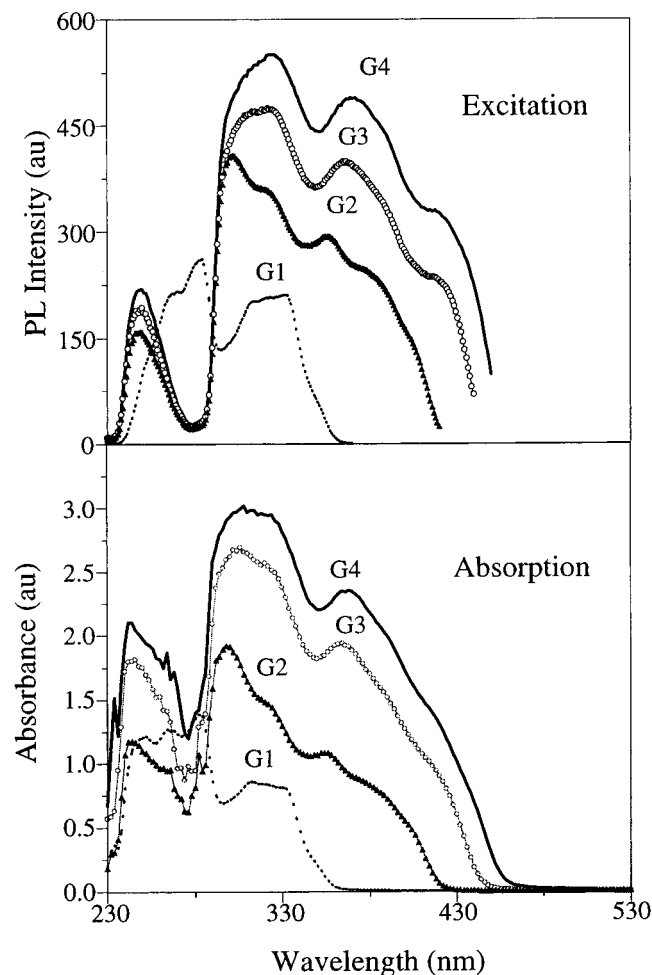


Figure 3. UV/vis absorption (bottom) and excitation (top) spectra of **G1–G4** in chloroform solutions.

through-bond charge-transfer mechanism. Even where the energy transfer occurs through space via a multistep hopping mechanism,³ notably fewer hopping steps might be required for the energy to transfer from the periphery to the center core. In addition, this type of dendrimer covers a much broader absorption range than meta-linked dendrimers. **G4**, for example, absorbs strongly from 240 nm all the way to 430 nm. Thus, the energy utilization efficiency in a light-harvesting application will be significantly improved in our dendrimers.

Due to the meta and para linkages, different branches in our dendrimers have varied conjugation lengths, which accounts for the broad absorption spectra. The energy transfer from the shorter conjugation-length branches to the most extended conjugation arm is expected. As shown in Figure 4, the fluorescence emission is red-shifted with higher generation dendrimers. The maximum emission wavelengths for **G2**, **G3**, and **G4** are 418, 441, and 455 nm, respectively. For a given dendrimer, only the emissions from the longest conjugated segment are observed. As shown in Figure 4 (top), whether the excitation wavelength is 250, 300, or 430 nm, the same emission maximum and the same emission edge are obtained. The emissions from **G4** are clearly independent of the excitation wavelengths. The excitation spectra of the dendrimers are also similar to their absorption spectra, as shown in Figure 3 (top). These results indicate an efficient energy transfer from the higher band-gap branches to the lowest band-gap branches. Due to the severe overlap of the absorption of the lowest band-gap branch with that of other branches, quantitative energy transfer efficiency cannot be obtained. We are currently attaching other

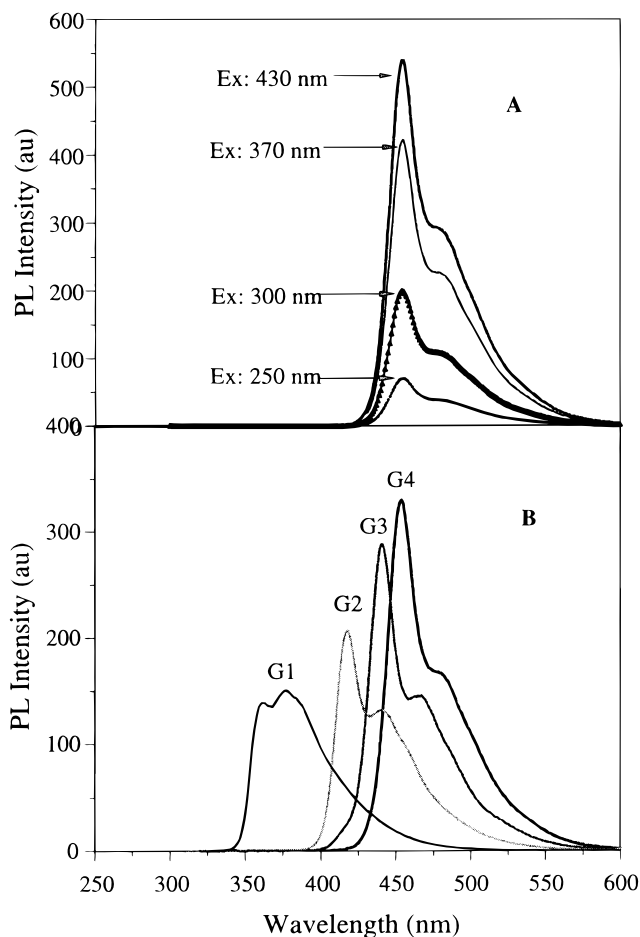


Figure 4. Fluorescence spectra (B) of **G1–G4** in dilute chloroform solutions. The top figure (A) shows the fluorescence spectra of **G4** under different excitation wavelengths.

energy acceptors with absorption wavelengths well separated from the absorptions of the dendrimers to further explore the excitation energy transfer process.

It is worth noting that, besides the application as efficient light-harvesting antennae, many other functional materials may be envisioned for our unsymmetrical dendrimers. Taking advantage of the phenol functional group at the dendritic locus, a variety of structural units with interesting properties can be anchored to the dendritic core.⁹ Work in this area is underway in our laboratory.

Conclusion

In conclusion, we have synthesized a new type of conjugated dendrimer using a rather simple approach that involves only one synthon and two sets of reaction conditions. This dendrimer possesses extended conjugation beyond its repeating units and shows efficient energy transfer from higher band-gap branches to the longest conjugated segment.

Acknowledgment. This work is supported by the Defense Advanced Research Projects Agency, Research Corporation, and the University of Missouri Research Board. We thank Ms. Kenna K. Hyatt and Ms. Florence Middleton for their assistance in preparing this manuscript.

JA0006907

(9) Our preliminary studies have shown that the core phenolic oxygen is accessible as a nucleophile for S_N2 reactions. For example, **G3** or **G4** can react with 1-pyrenemethanol, resulting in pyrene-anchored dendrimers.